Supporting information for:

Stronger or weaker acid, which is more efficient for the catalytic performance of Beckmann rearrangement reaction over solid acids?

Yueying Chu,[a] Peng Ji,[b] Xianfeng Yi,[a] Shenhui Li,[a] Peng Wu,[b] Anmin Zheng,* [a] Feng Deng*[a]

a, State Key Laboratory of Magnetic Resonance and Atomic and Molecular Physics, Natioanl Center for Magnetic Resonance in Wuhan, Wuhan Institute of Physics and Mathematics, Chinese Academy of Sciences, Wuhan 430071 (P.R. China)

b, Shanghai Key Laboratory of Green Chemistry and Chemical Processes, Department of Chemistry, East China Normal University, Shanghai 200062 (P.R. China)

c. Hubei Key Laboratory for Processing and Application of Catalytic Materials, Huanggang Normal University, Huanggang 438000 (P.R. China)

Synthesis of ZSM-5-type zeolites:

Silicalite-1: The synthesis of B-MFI was performed according to Ref 1[1]. Firstly, the required amount of TEOS was added in the TPAOH aqueous solution under stirring. Ethanol formed from the hydrolysis of TEOS was removed by evaporation at 353 K to form a synthetic gel having the following molar composition: 1.0 SiO_2: 0.4 TPAOH: 15 H_2O.

B-ZSM-5: The synthesis of B-MFI was performed according to Ref 2[2]. H_3BO_3 was dissolved in TPAOH aqueous solution under stirring, and the mixture was stirred vigorously at room temperature for 30 min to become clear, then required amount of TEOS was added. The formed ethanol was removed by evaporation at 353 K to form a synthetic gel having the following molar composition: 1.0 SiO_2: 0.03 H_3BO_3: 1.0 TPAOH: 28 H_2O.

Al-ZSM-5: Na-ZSM-5 was firstly prepared using a seeding method according to Ref 3[3]. The colloidal silicalite-1 seed with a uniform crystal size of 60 nm was prepared according to the procedures described in Ref 4[4]. NaOH and sodium aluminate were dissolved in TPAOH aqueous solution under stirring, then the required amount of colloidal silica was added to form a synthetic gel having the following molar composition: 1.0 SiO_2: 0.015 Al_2O_3: 0.02 Na_2O: 0.15 TPAOH: 20 H_2O. Lastly, the silicalite-1 seed, corresponding to 0.5 wt.% of the silica in gel, was added to the mixed gel. Na-ZSM-5 was first converted into NH_4-ZSM-5 by 4-fold ion exchange with 2.0 M aqueous solution of NH_4NO_3 at 353 K for 12 h. After each exchange, the sample was washed with excessive deionized water and was isolated by filtration. The sample was finally dried at 353 K overnight, and NH_4-ZSM-5 was obtained. NH_4-ZSM-5 was then calcinated at 773 K in the tube furnace with flowing dry air for 3 h to get the H-ZSM-5 catalyst.

Synthesis of MCM-41-type zeolites

MCM-41-type zeolites were synthesized according to the previous work[5,6]. In a typical synthesis of MCM-41: 0.8 g of CTAB was dissolved in 25mL of water with 12 mL $NH_3 \cdot H_2O$, followed by the addition of 4.5 mL TEOS. After stirring at room

temperature for 5-6 h, the mixture was transferred into an autoclave for further condensation at various temperatures for 1 day. The product was collected by filtration, dried in air and calcined at 550°C to remove the surfactant.

To prepare B-MCM-41 and Al-MCM-41, a required amount of H_3BO_3 or aluminium isopropoxide was added together with TEOS.

References：

(1)   Kragten, D. D.; Fedeyko, J. M.; Sawant, K. R.; Rimer, J. D.; Vlachos, D. G.; Lobo, R. F.; Tsapatsis, M. *J. Phys. Chem. B* **2003**, *107*, 10006.

(2)   Alshebani, A.; Pera-Titus, M.; Landrivon, E.; Schiestel, T.; Miachon, S.; Dalmon, J. A. *Microporous Mesoporous Mater.* **2008**, *115*, 197.

(3)   Xu, F.; Dong, M.; Gou, W.; Li, J.; Qin, Z.; Wang, J.; Fan, W. *Microporous Mesoporous Mater.* **2012**, *163*, 192.

(4)   Li, Q.; Hedlund, J.; Sterte, J.; Creaser, D.; Bons, A.-J. *Microporous Mesoporous Mater.* **2002**, *56*, 291.

(5)   Ying, J. Y.; Mehnert, C. P.; Wong, M. S. *Angew. Chem. Int. Edit.* **1999**, *38*, 56.

(6)   Chen, C. Y.; Li, H. X.; Davis, M. E. *Microporous Mater.* **1993**, *2*, 17.

Table of Contents

2.25; (f), 2.50 Å. Selected interatomic distances (in Å) are indicated.

Figure S4. Optimized geometries of transition state (TS3) for the tautomerization step of cyclohexanone oxime reaction on the isolated Brønsted acid site models with various terminal Si–H bond length r_{Si-H}: (a), 1.30; (b), 1.47; (c), 1.75; (d), 2.00; (e), 2.25; (f), 2.50 Å. Selected interatomic distances (in Å) are indicated.

Figure S5. Optimized geometries of transition state (TS1) for the 1,2-H shift step of acetoxime reaction on the isolated Brønsted acid site models with various terminal Si–H bond length r_{Si-H}: (a), 1.30; (b), 1.47; (c), 1.75; (d), 2.00; (e), 2.25; (f), 2.50 Å. Selected interatomic distances (in Å) are indicated.

Figure S6. Optimized geometries of transition state (TS2) for the rearrangement step of acetoxime reaction on the isolated Brønsted acid site models with various terminal Si–H bond length r_{Si-H}: (a), 1.30; (b), 1.47; (c), 1.75; (d), 2.00; (e), 2.25; (f), 2.50 Å. Selected interatomic distances (in Å) are indicated.

Figure S7. Optimized geometries of transition state (TS3) for the tautomerization step of acetoxime reaction on the isolated Brønsted acid site models with various terminal Si–H bond length r_{Si-H}: (a), 1.30; (b), 1.47; (c), 1.75; (d), 2.00; (e), 2.25; (f), 2.50 Å. Selected interatomic distances (in Å) are indicated.

Figure S8. Optimized geometries of transition states (TS) for cyclohexanone oxime (a, b, c) and acetoxime (d, e, f) Beckmann rearrangement reaction on the 72T H-ZSM-5 extend model. (a) and (d), 1,2-H shift step; (b) and (e), rearrangement step; (c) and (f), tautomerization step. Selected interatomic distances (in Å) are indicated.

Table S1. Textural properties of ZSM-5 and MCM-41 zeolites.

| catalysts	BET surface area (m^2g^{-1})	External surface area ($m^2 g^{-1}$)	Mesopore volume ($cm^3 g^{-1}$)	Micropore volume ($cm^3 g^{-1}$)
Si-ZSM-5	335	12	0.054	0.176
B-ZSM-5	351	13	0.047	0.182
Al-ZSM-5	326	16	0.051	0.166
Si-MCM-41	1023	852	0.767	0.109
B-MCM-41	1055	885	0.763	0.116
Al-MCM-41	992	844	0.757	0.112

Table S2: Activation Energies (kcal/mol) and Mulliken charges (|e|) on the hydrogencarbon fragments of reactant (Rea), transition state (TS) and intermediate (Int) for cyclohexanone oxime Beckmann rearrangement reaction on the isolated Brønsted acid site models with terminal Si−H bond distance from 1.30 to 2.75 Å. (see scheme 1)

| r_{Si-H}	Energy	Activation Energies			Net charge					
	DPE	E_{act1}	E_{act2}	E_{act3}	Rea	TS1	Int1	TS2	Int2	TS3
1.30	319.2	13.5	38.9	25.0	0.74	0.41	0.48	0.81	0.47	0.53
1.47	309.6	15.5	35.8	24.3	0.76	0.43	0.50	0.83	0.49	0.58
1.75	293.2	19.1	30.3	22.9	0.79	0.46	0.55	0.86	0.52	0.81
2.00	280.1	22.1	25.7	19.9	0.81	0.48	0.59	0.88	0.55	0.83
2.25	269.4	28.2	21.7	17.5	0.85	0.50	0.63	0.90	0.57	0.85
2.50	260.8	29.9	19.3	15.7	0.90	0.51	0.82	0.91	0.59	0.85
2.75	253.5	34.7	17.5	14.4	0.73	0.51	0.83	0.90	0.61	0.85

Table S3: Activation Energies (kcal/mol) and Mulliken charges (|e|) on the hydrogencarbon fragments of reactant (Rea), transition state (TS) and intermediate (Int) for acetoxime Beckmann rearrangement reaction on the isolated Brønsted acid site models with terminal Si−H bond distance from 1.30 to 2.75 Å. (see scheme 1)

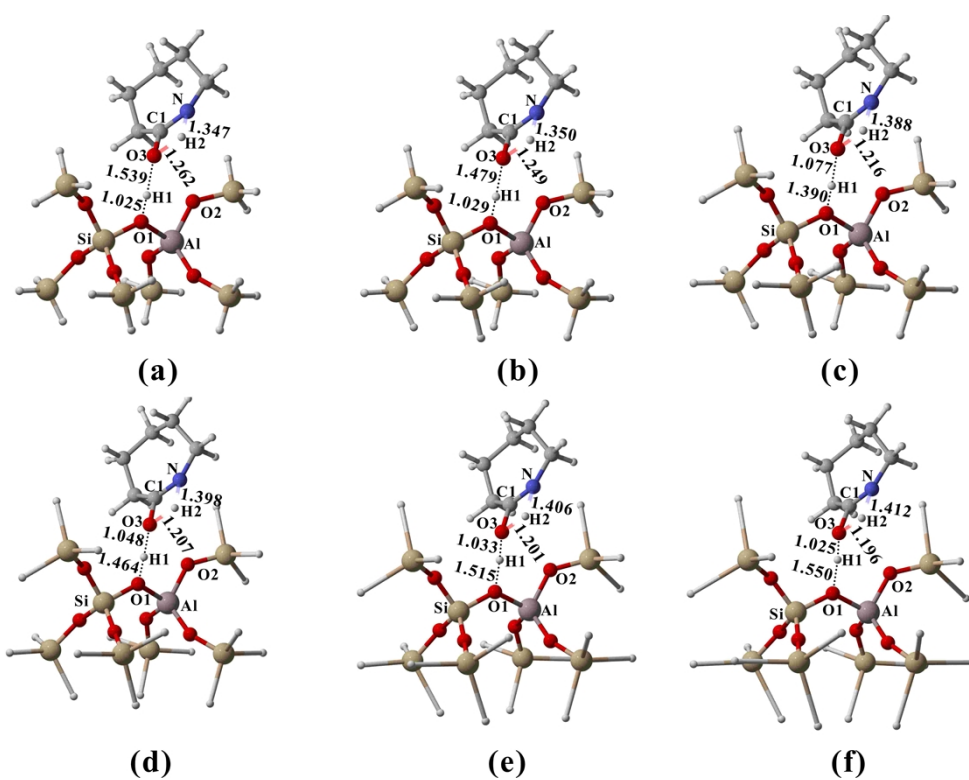| r_{Si-H}	Energy	Activation Energies			Net charge					
	DPE	E_{act1}	E_{act2}	E_{act3}	Rea	TS1	Int1	TS2	Int2	TS3
1.30	319.2	13.8	39.2	25.3	0.74	0.42	0.48	0.78	0.48	0.55
1.47	309.6	15.7	38.0	24.7	0.76	0.44	0.50	0.79	0.48	0.57
1.75	293.2	19.1	32.8	23.3	0.79	0.46	0.54	0.85	0.52	0.63
2.00	280.1	22.0	26.3	21.2	0.81	0.48	0.59	0.85	0.55	0.83
2.25	269.4	24.2	22.1	18.7	0.83	0.50	0.78	0.85	0.58	0.84
2.50	260.8	28.7	19.3	16.7	0.85	0.50	0.81	0.83	0.59	0.84
2.75	253.5	33.4	16.5	15.0	0.74	0.51	0.82	0.84	0.60	0.83
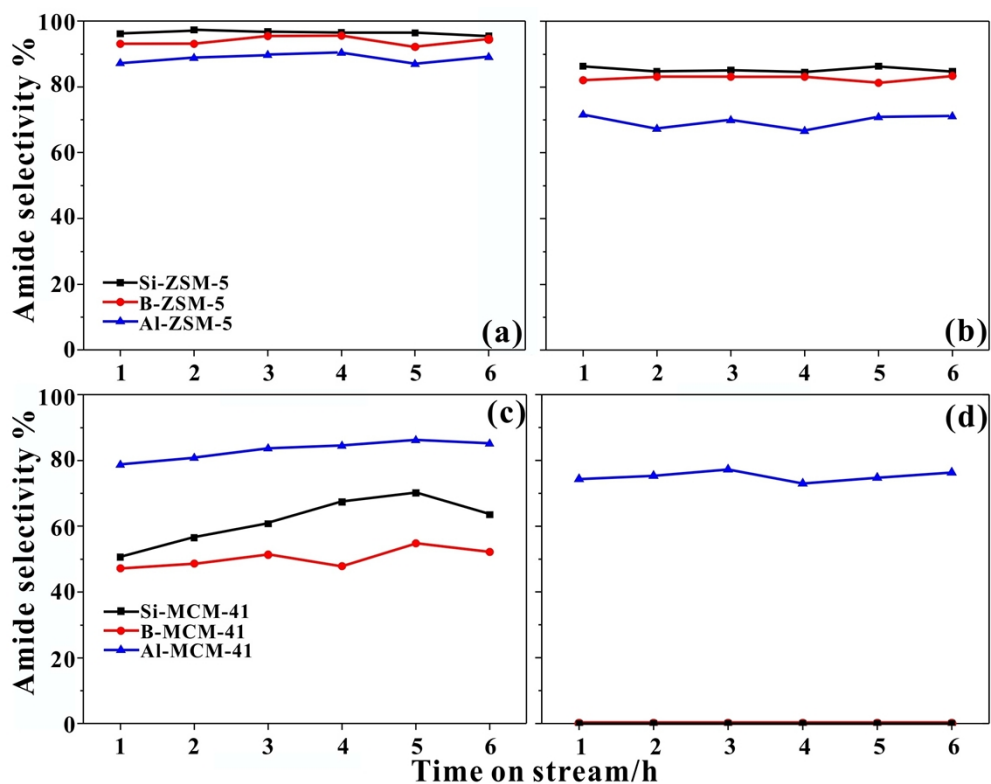
Figure S1. The BR reaction selectivity of cyclohexanone oxime (a,c) and acetoxime (b,d) as a function of time on stream over MFI-type (a,b) and MCM-14-type (c,d) zeolites with varied Brønsted acid strengths at 633 K (for cyclohexanone oxime) and 653K (for acetone oxime).
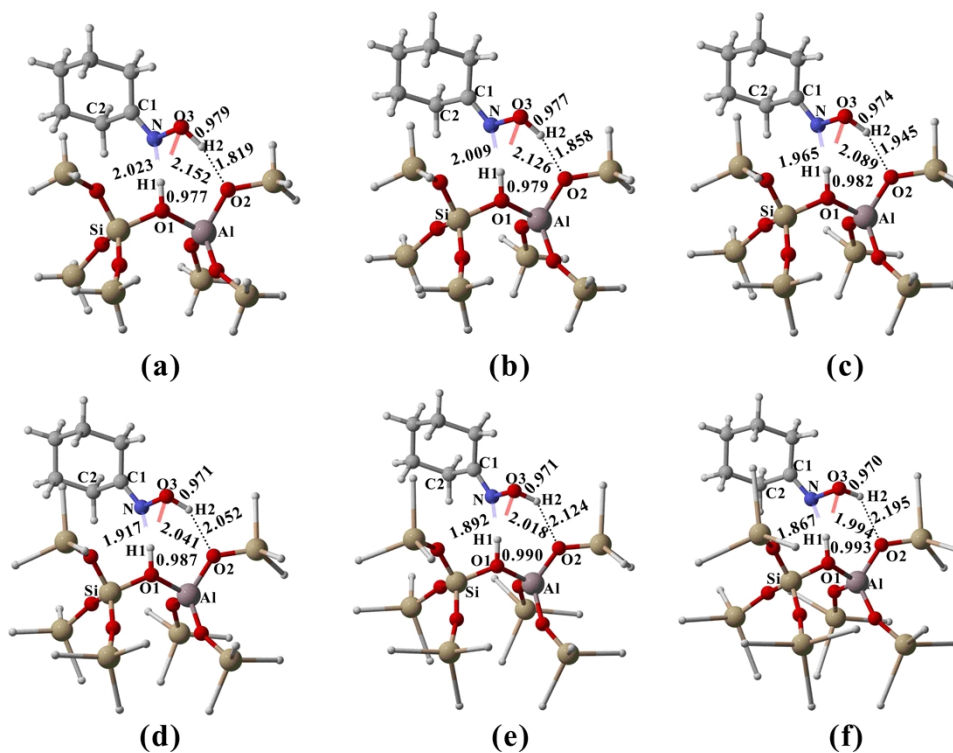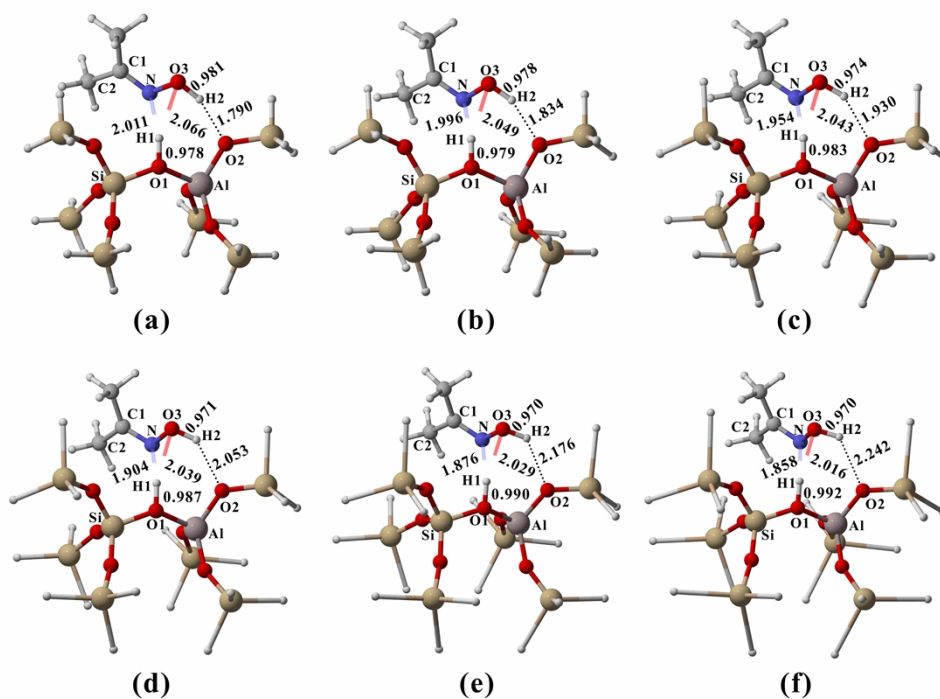
Figure S2. Optimized geometries of transition state (TS1) for the 1,2-H shift step of cyclohexanone oxime reaction on the isolated Brønsted acid site models with various terminal Si–H bond length r_{Si-H}: (a), 1.30; (b), 1.47; (c), 1.75; (d), 2.00; (e), 2.25; (f), 2.50 Å. Selected interatomic distances (in Å) are indicated.
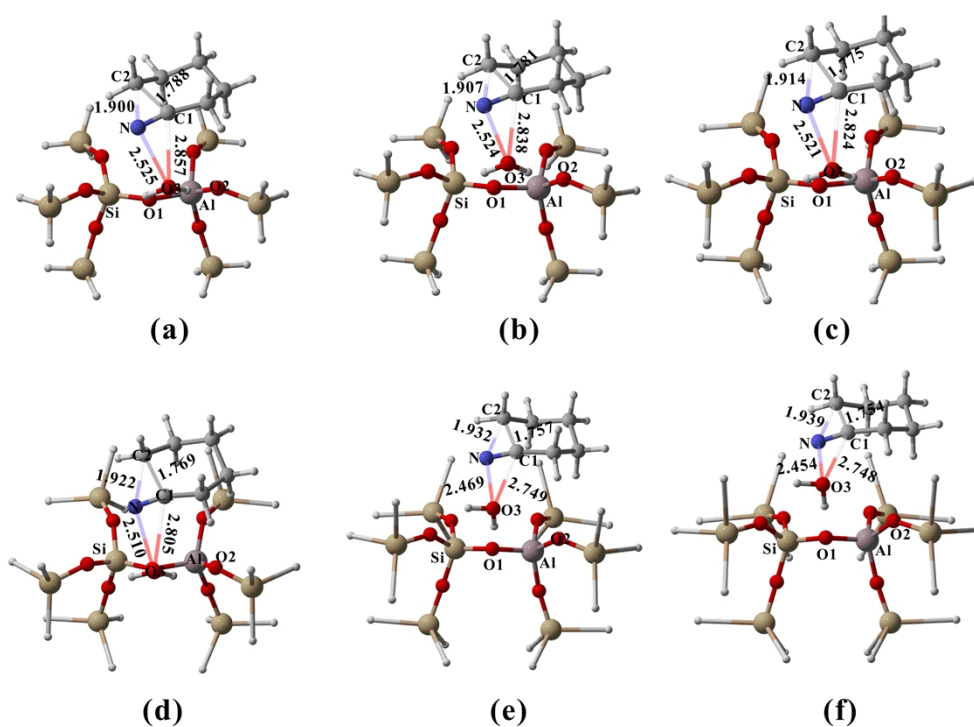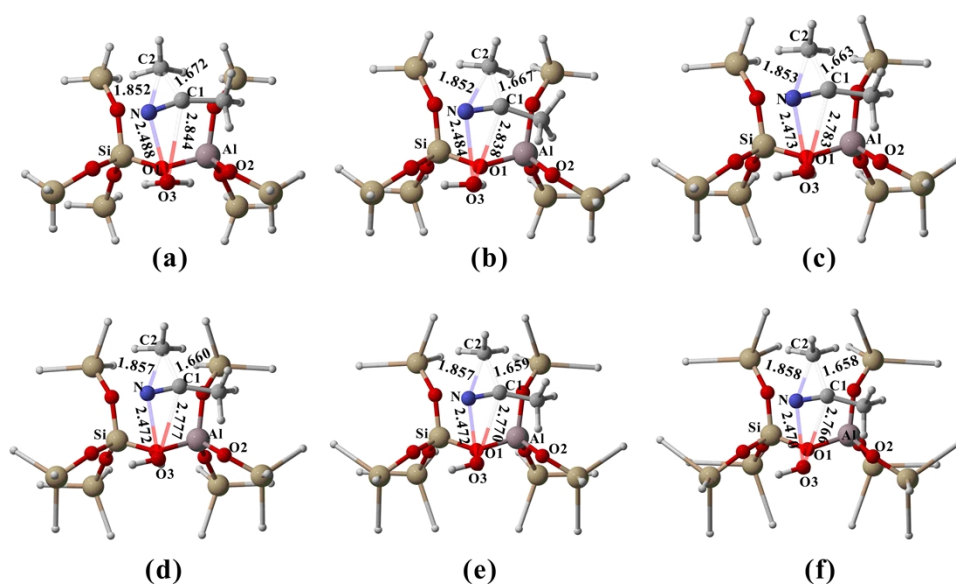
Figure S3. Optimized geometries of transition state (TS2) for the rearrangement step of cyclohexanone oxime reaction on the isolated Brønsted acid site models with various terminal Si–H bond length r_{Si-H}: (a), 1.30; (b), 1.47; (c), 1.75; (d), 2.00; (e), 2.25; (f), 2.50 Å. Selected interatomic distances (in Å) are indicated.

Figure S4. Optimized geometries of transition state (TS3) for the tautomerization step of cyclohexanone oxime reaction on the isolated Brønsted acid site models with various terminal Si–H bond length r_{Si-H}: (a), 1.30; (b), 1.47; (c), 1.75; (d), 2.00; (e), 2.25; (f), 2.50 Å. Selected interatomic distances (in Å) are indicated.

Figure S5. Optimized geometries of transition state (TS1) for the 1,2-H shift step of acetoxime reaction on the isolated Brønsted acid site models with various terminal Si–H bond length $r_{\text{Si-H}}$: (a), 1.30; (b), 1.47; (c), 1.75; (d), 2.00; (e), 2.25; (f), 2.50 Å. Selected interatomic distances (in Å) are indicated.
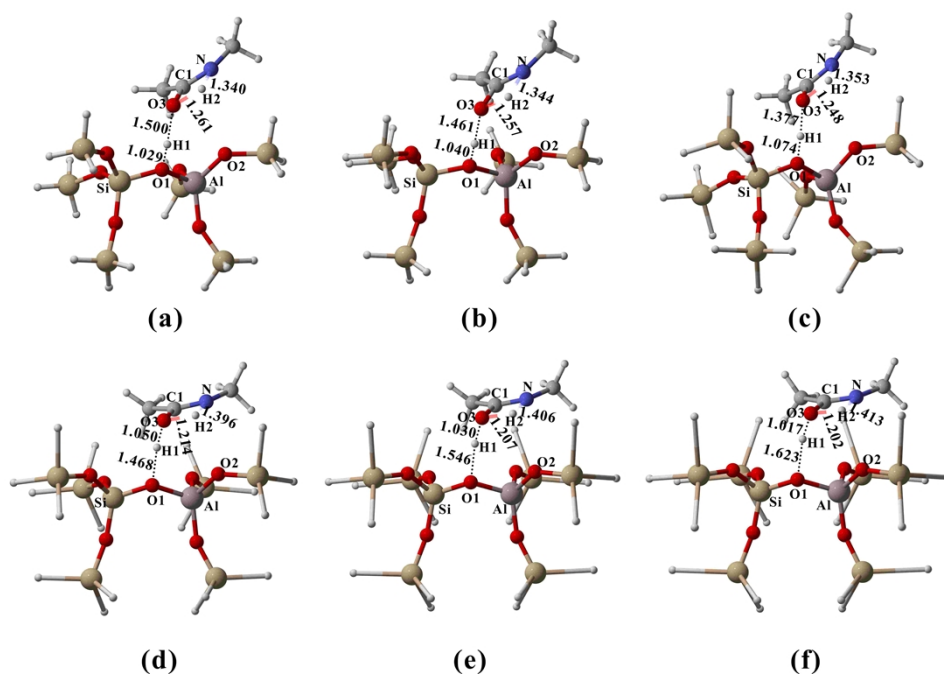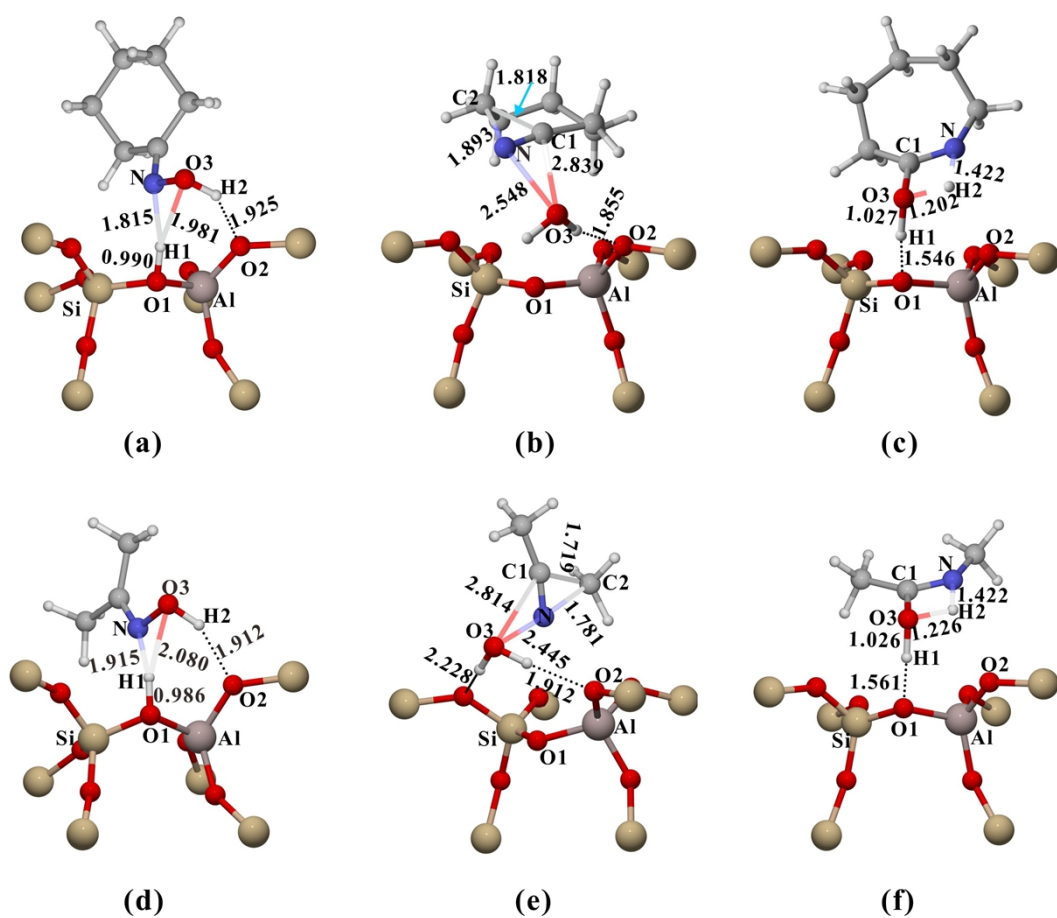
Figure S6. Optimized geometries of transition state (TS2) for the rearrangement step of acetoxime reaction on the isolated Brønsted acid site models with various terminal Si–H bond length r_{Si-H}: (a), 1.30; (b), 1.47; (c), 1.75; (d), 2.00; (e), 2.25; (f), 2.50 Å. Selected interatomic distances (in Å) are indicated.

Figure S7. Optimized geometries of transition state (TS3) for the tautomerization step of acetoxime reaction on the isolated Brønsted acid site models with various terminal Si–H bond length r_{Si-H}: (a), 1.30; (b), 1.47; (c), 1.75; (d), 2.00; (e), 2.25; (f), 2.50 Å. Selected interatomic distances (in Å) are indicated.

Figure S8. Optimized geometries of transition state for the cyclehexanone oxime (a, b, c) and acetoxime (d, e, f) reaction over the 72T model with complete H-ZSM-5 double 10-MR pore structure. Selected interatomic distances (in Å) are indicated.